Supplementary Information

Construction of a redox-active metal−organic framework with an octanuclear lithium one-dimensional building block

Shu-Fan Li,[a] Ya-Ru Meng,[a] Min-Jie Xu,[a] Gen Zhang*[a] and Jian Su,*[a]

[a] School of Chemical Engineering, Nanjing University of Science and Technology, Nanjing, Jiangsu 210094, China.

E-mail: *zhanggen@njust.edu.cn; sujian@njust.edu.cn*

Experimental Procedures

Materials and Characterization

Materials.

All the chemicals are commercially available, and used without further purification. $LiNO_3$ (Shanghai Macklin Biochemical Co., Ltd), N, N, N', N'-tetrakis(4-carboxyphenyl)-1,4-phenylenediamine (H_4TCPPDA) (97%, Shanghai Tengqian Biotechnology Co., Ltd), CH_3OH (Shanghai Aladdin Biochemical Technology Co., Ltd.), N, N-dimethylformamide (DMF) (Nanjing reagent Co., Ltd), and H_2O (Deionized water).

Characterization.

Powder X-ray diffraction (PXRD): PXRD patterns were acquired on a Bruker D8 ADVANCE diffractometer at room temperature.

Fourier transform infrared (FT-IR): IR spectra were measured on a Thermo Fisher Scientific Optics NICOLETIS20.

Scanning electron microscope (SEM): SEM images were collected using a JSM-7800F PRIME system.

Transmission electron microscope (TEM): TEM images were obtained with a JEM-2100Plus, JEOL.

Thermogravimetric analysis (TGA): TGA were recorded on TGA/SDTA851E under flowing N_2 with 10 K min^{-1} ramp rate.

Ultraviolet-visible-near-infrared light absorption spectra (UV-vis-NIR): The UV-vis spectra were collected using EVOLUTION220.

Electron paramagnetic resonance (EPR): The EPR spectra were obtained with a Bruker EMX-10/12 X-band (Li_8-MOF and Ag NPs@Li_8-MOF) and EPR200-Plus (Li_8-MOF recorded during spectroelectrochemistry) at room temperature.

X-ray photoelectron spectroscopy (XPS): The xps data were tested by PHI QUANTERA II (Japan vacuum) instrument. X-ray photoelectron spectrometer using standard and monochromatic Al Kα radiation. The binding energies from the spectra were calibrated against the C 1s peak located at 284.6 eV.

Cyclic voltammetry (CV) and **differential pulse voltammetry** (DPV): The CV and DPV data were obtained by using a CH Instrument CHI760E electrochemical Analyzer. Measurements were performed in a three-electrode system. Glassy carbon was used as the working electrode, platinum wire as an auxiliary electrode and Ag/AgCl as a reference electrode. The Li_8-MOF was grinded and coated on glassy carbon electrode. The electrolyte is 0.1 M $(C_2H_5)_4N^+PF_6^-$/DMF.

Spectroelectrochemistry: Spectroelectrochemistry spectra results of Li_8-MOF on ITO were obtained by CHI760E electrochemical Analyzer and UV−Vis spectrometer EVOLUTION220. Measurements were performed in a three-electrode system (Figure S23) and the electrolyte is 0.1 M $(C_2H_5)_4N^+PF_6^-$/DMF.

Synthesis of Li_8-MOF.

$LiNO_3$ (15 mg, 0.218 mmol) and $H_4TCPPDA$ (5 mg, 0.008 mmol) were disolved with N, N-dimethylformamide (DMF, 1.5 mL) and H_2O (0.25 mL) in a 10 mL glass vial. The vial was sonicated for 5 min and incubated at 135 °C for 3 days. The light yellow strip crystals were crystallized and collected by filtration (based on 75 % yield of $H_4TCPPDA$). Analysis calcd (%) for $C_{77}H_{61}Li_8N_7O_{19}$: C 64.05; H 4.26; N 6.79. Found: C 57.97; H 4.15; N 6.13. It is well known that MOFs, as porous crystalline materials, trap guest molecules. Therefore, it is difficult to fit the EA data accurately. [1] FT-IR (cm^{-1}): 1674 (s), 1635 (w), 1589 (vs), 1540 (m), 1502 (s), 1386 (vs), 1303 (m), 1258 (m), 1176 (m), 1147 (w), 1101 (s), 1062 (vw), 1014 (vw), 960 (vw), 923 (vw), 841 (m), 785 (vs), 705 (s), 672 (s), 634 (w), 566 (w), 541(w).

Fabrication of electrode (Li_8-MOF on ITO glass).

Take 10 mg of Li_8-MOF for grinding, then add 200 μL of dichloromethane, sonicate for 20 minutes and leave it to stand. Clean the ITO glass substrate (size 2 × 1 cm) by immersing it in petroleum ether, acetone, and ethanol, followed by sonication for 20 minutes. Apply the top layer of the suspension onto the ITO glass and and allow it to dry at room temperature.

Single Crystal Structure Studies.

Single-crystal X-ray diffraction intensity data was collected on a Bruker D8 Quest single-crystal X-ray diffractometer outfitted with a PHOTON-3 CMOS detector using Incoatec IμS microfocus Mo source (3rd generation) (λ= 0.71073 Å) at 200 K. The raw data collection, transformation, and reduction were accomplished by APEX3 software[2]. Adsorption corrections were carried out using the SADABS routine. The structures were solved by direct methods and refined by full-matrix least-squares on F^2 using the SHELXTL software package[3]. Non-hydrogen atoms were refined with anisotropic displacement parameters during the final cycles. Hydrogen atoms of $TCPPDA^{4-}$ were positioned at calculated ideal positions with isotropic displacement parameters. The free solvent molecules were highly disordered and impossible to locate and refine. The diffuse electron densities resulting from these residual solvent molecules were removed from the data set using the SQUEEZE routine of PLATON and refined further using the data generated[4]. The solvent contents are not represented in the unit cell formula in the crystal data. The final formula of Li_8-MOF was calculated from the SQUEEZE results, charge balance, and TGA data. The X-ray crystallographic coordinates for structures reported in this article have been deposited at the Cambridge Crystallographic Data Centre (CCDC), under deposition numbers CCDC 2351585 for compounds Li_8-MOF. These data can be obtained free of charge from the Cambridge Crystallographic Data Centre via www.ccdc.cam.ac.uk/data_request/cif. All relevant data supporting the findings of this study are available from the corresponding authors upon request

Table S1 Selected bond lengths (Å) and angles (°) of Li_8-MOF.

O1-Li3	1.834(9)	O2-Li1	1.933(6)
O2-Li2	1.916(6)	O3-Li1	1.898(7)
O4-Li3[1]	1.937(9)	O4-Li4	1.932(7)
O5-Li2[2]	1.926(6)	Li3-O10	2.544(17)
O5-Li3[2]	2.453(14)	Li4-O6[5]	1.995(7)
O5-Li4[3]	1.999(6)	O8-Li4[6]	1.919(7)
O6-Li3[4]	1.932(9)	O8-Li2[7]	1.924(6)
O6-Li4[5]	1.995(7)	Li1-O9	1.962(7)
Li2-O5[2]	1.926(6)	O7-Li2[6]	1.938(6)
O7-Li1[6]	1.960(7)	O1-Li3 -O5[2]	102.2(5)
O1-Li3 -O10	82.6(5)	O1-Li3 -O6[10]	123.7(5)
O3-Li1 -O7[8]	116.2(3)	O4-Li4-O6[5]	105.6(3)
O3-Li1 -O9	106.6(3)	O4[9]-Li3-O5[2]	93.1(5)
O7[8]-Li1-O9	108.2(3)	O4[9]-Li3-O10	88.9(5)
O2-Li2-O5[2]	115.5(3)	O6[5]-Li4-O5[11]	101.0(3)
O2-Li2-O7[8]	92.9(3)	O8[8]-Li4-O4	131.7(3)
O2-Li2-O8[7]	113.3(3)	O5[2]-Li3-O10	172.3(5)
O5[2]-Li2-O7[8]	122.8(3)	O6[10]-Li3-O4[9]	109.5(4)
O8[7]-Li2-O5[2]	92.5(3)	O6[10]-Li3-O5[2]	88.5(4)
O8[7]-Li2-O7[8]	121.6(3)	O6[10]-Li3-O10	83.8(5)
O1-Li3 -O4[9]	124.6(5)	O4-Li4-O5[11]	117.2(3)
O2-Li1 -O7[8]	91.8(3)	O2-Li1 -O9	106.2(3)
O3-Li1-O2	126.4(4)	O8[8]-Li4-O6[5]	106.9(3)
O8[8]-Li4-O5[11]	90.4(3)		

Symmetry codes: [1] -1+X,+Y,+Z; [2] 1-X,1-Y,2-Z; [3] +X,1+Y,+Z; [4] -1+X,1+Y,+Z; [5] -X,1-Y,2-Z; [6] +X,+Y,-1+Z; [7] 1-X,-Y,1-Z; [8] +X,+Y,1+Z; [9] 1+X,+Y,+Z; [10] 1+X,-1+Y,+Z; [11] +X,-1+Y,+Z.

Table S2 Crystal data and structure refinements for Li_8-MOF.

	Li_8-MOF
Empirical formula	$2(C_{34}H_{20}Li_4N_2O_8)$, $3(C_3H_7NO)$
Formula weight	1443.84
Temperature (K)	200
Crystal system	triclinic
Wavelength (Å)	0.71073
Space group	*P-1*
a (Å)	9.8956(6)
b (Å)	13.8451(9)
c (Å)	14.4170(9)
α (°)	95.736(2)
β (°)	94.844(2)
γ (°)	102.727(2)
Volume ($Å^3$)	1905.5(2)
Z	1
Calculated density (gcm^{-3})	1.258
F(000)	748.0
Absorption coe. μ/mm^{-1}	0.089
No. of reflections measured	28945
No. of independent reflections	6261
θ (°)	1.954 - 24.420
R_{int}	0.0691
R_1, wR_2 [I ≥2σ (I)]	0.0664 / 0.1979
R_1, wR_2 [all data]	0.0874 / 0.2200
GOF	1.045
Largest diff. peak and hole ($eÅ^{-3}$)	1.023 / -0.388
CCDC number	2351585

Table S3 Composition of SBUs and ligands of Li-MOF.

name	SBU	ligand	ref
IMP-22	1D Li_8-based SBU	Di-carboxylic acid	5
IMP-24	Right-handed helical Li^+-based chains	Tri-carboxylic acid	5
$[(Li^+)(C_6H_4NO_2^-)]$·0.5DMF	Chain consists of alternating four-membered rings and eight-membered rings	Mono-carboxylic acid	6
$[Li_2(H_2pml)]·C_4H_8O_2$ (1)	helical chain	Tetra- carboxylic acid	7
$[Li_2(H_2pml)]$ (2)	binuclear building unit	Tetra- carboxylic acid	7
$[Li(H_2tatab)]·5H_2O$ (3)	chain-like unit	Di-carboxylic acid	7
$(H_3O)[Li_{11}(H_2O)_5(Html)_6]·8C_4H_8O_2$ (4)	$\{Li_{11}\}$ unit	Tri-carboxylic acid	7
$[Li\{Li(nmp)\}\{Li(H_2O)(nmp)\}\{Li(nmp)_2\}_2(H_2tms)(Htms)_2]$·NMP·EtOH (5)	Binuclear and mononuclear unit	Tri-carboxylic acid	7
CPM-47	helical inorganic chains made of 4-membered and 6-membered rings	Mono-carboxylic acid	8
Li_2(hba)(DMF) (1)	chain	Mono-carboxylic acid	9
Li-NTA	$[Li_2O_4]$ unit	Di-carboxylic acid	10
Li_8-MOF	1D Li_8-based SBU	Tetra- carboxylic acid	This work

Results and Discussion

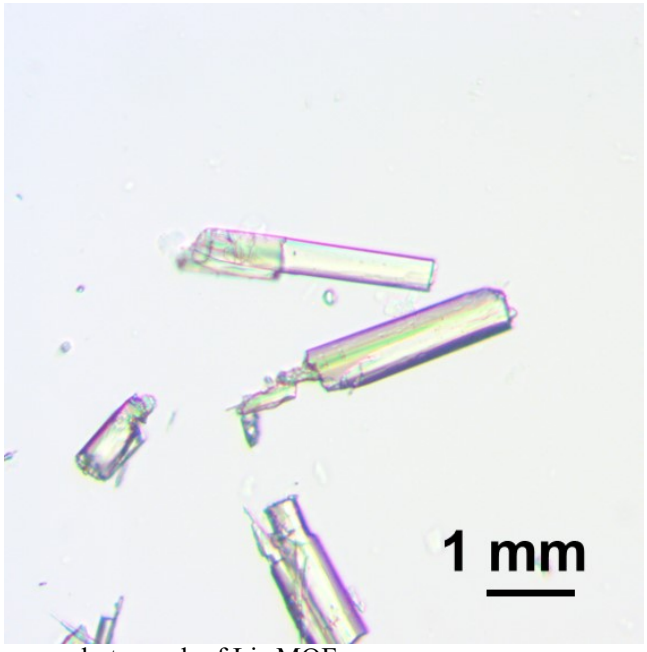

Figure S1. The Optical microscope photograph of Li_8-MOF.

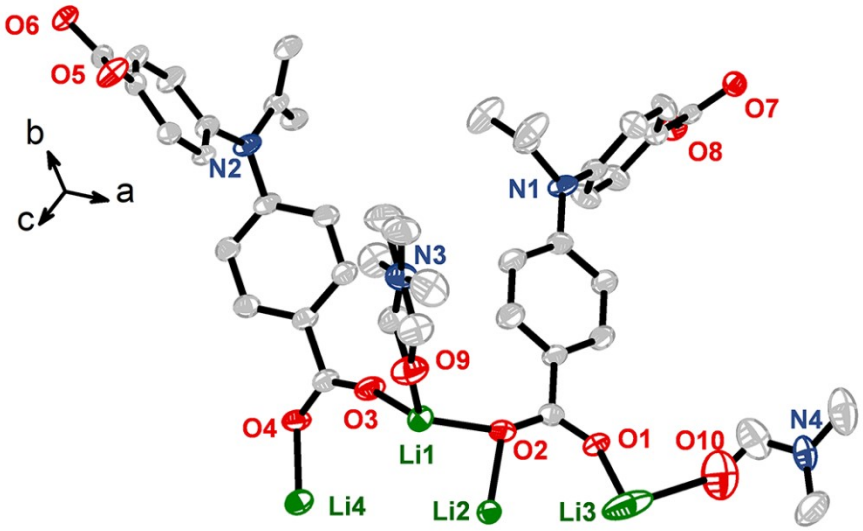

Figure S2. The asymmetric unit of Li_8-MOF. Displacement ellipsoids are drawn at the 50% probability level. Color scheme: Li, green; O, red; C, grey; N, dark blue. The hydrogen atoms are omitted for clarity. The DMF is disordered (where N3 is located). The DMF occupies 0.5 (where N4 is located).

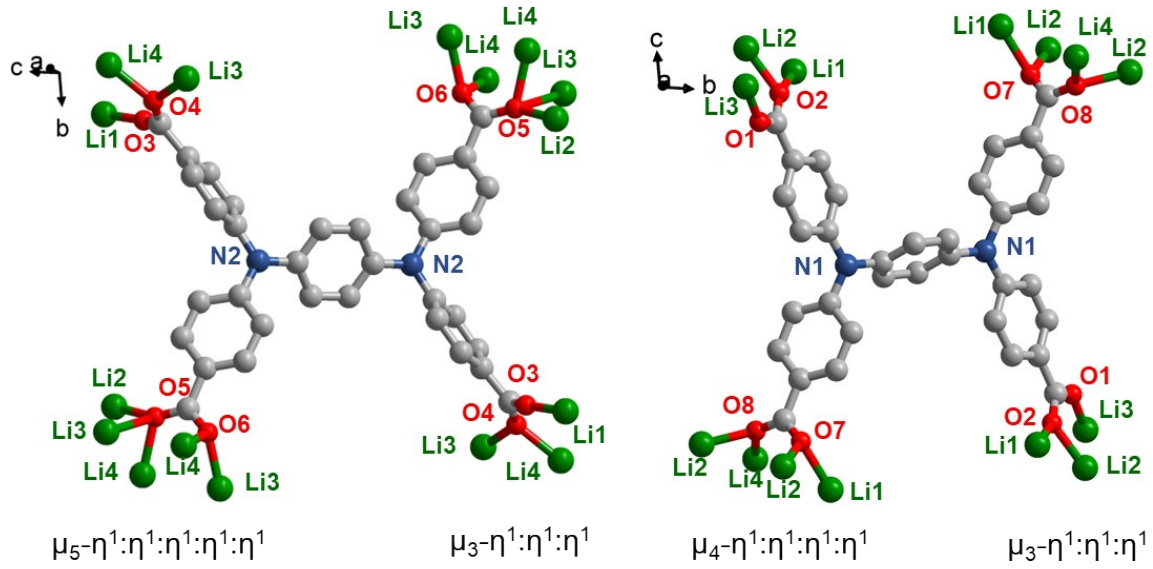

Figure S3. The coordination environments of $TCPPDA^{4-}$. Color scheme: Li, green; O, red; C, grey; N, dark blue. The hydrogen atoms are omitted for clarity.

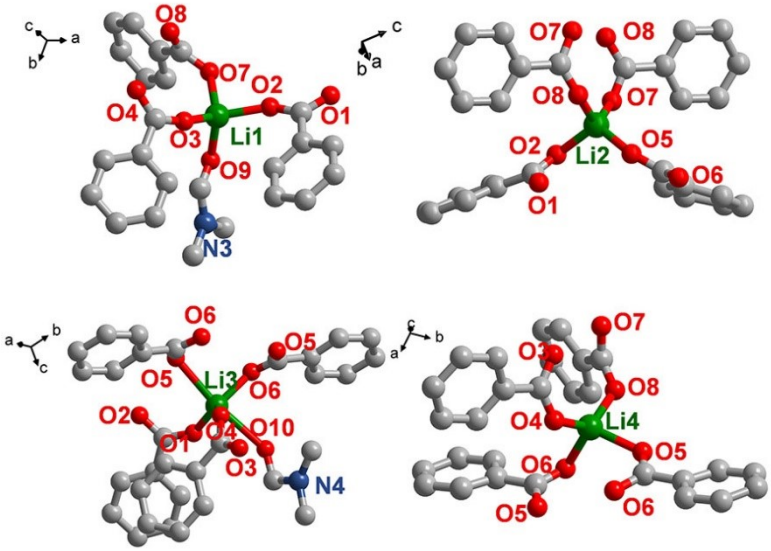

Figure S4. The coordination environment of Li^{+} ions. Color scheme: Li, green; O, red; C, grey; N, dark blue. The hydrogen atoms are omitted for clarity.

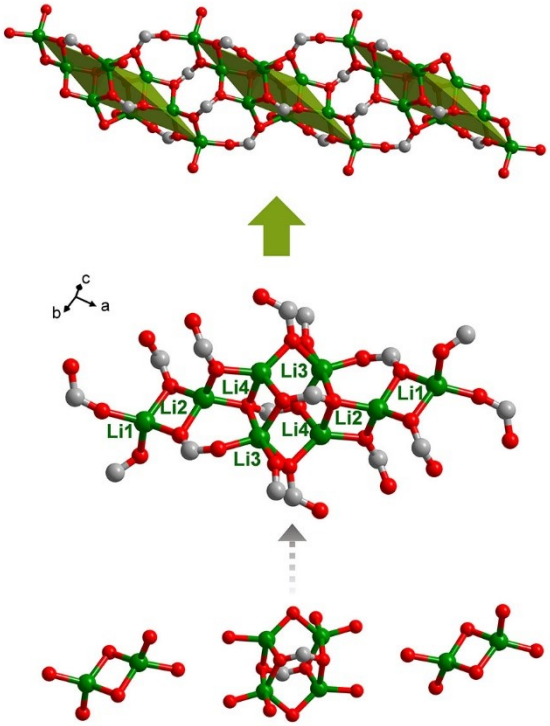

Figure S5. The octanuclear cluster and 1D rod SBU. Color scheme: Li, green; O, red; C, grey; N, dark blue. The hydrogen atoms are omitted for clarity.

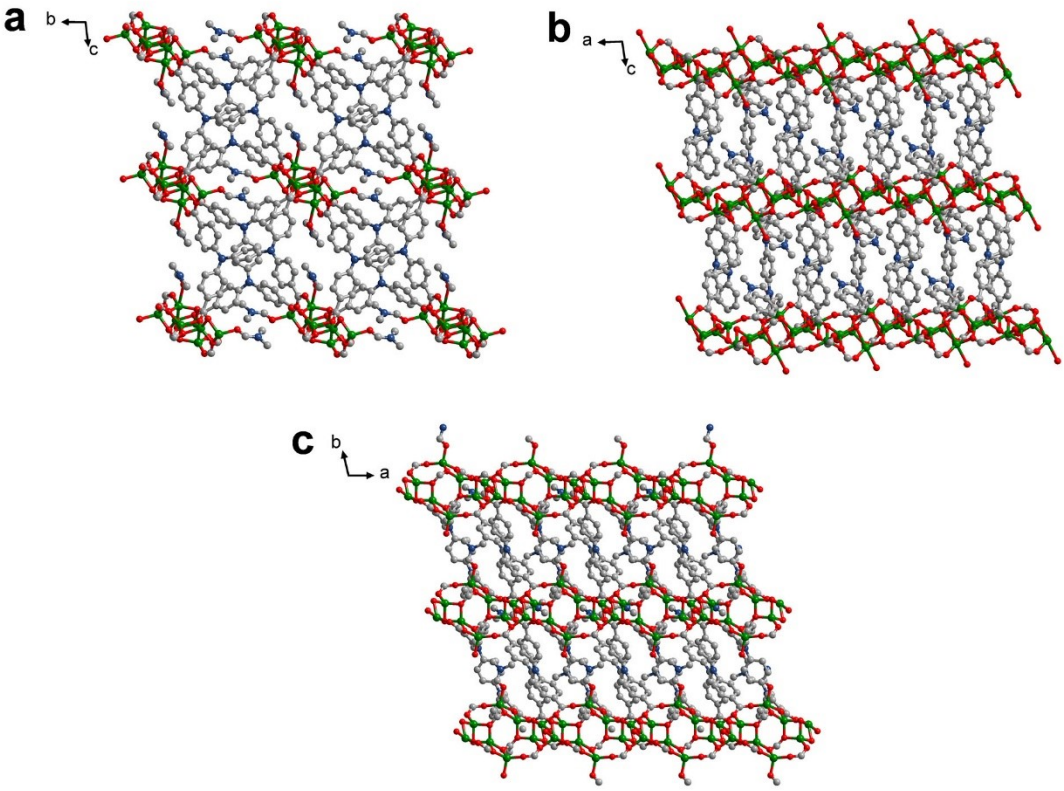

Figure S6. The 3D frameworks of Li_8-MOF are viewed in the (a) **a** axis, (b) **b** axis, and (c) **c** axis. Color scheme: Li, green; O, red; C, grey; N, dark blue. The hydrogen atoms are omitted for clarity.

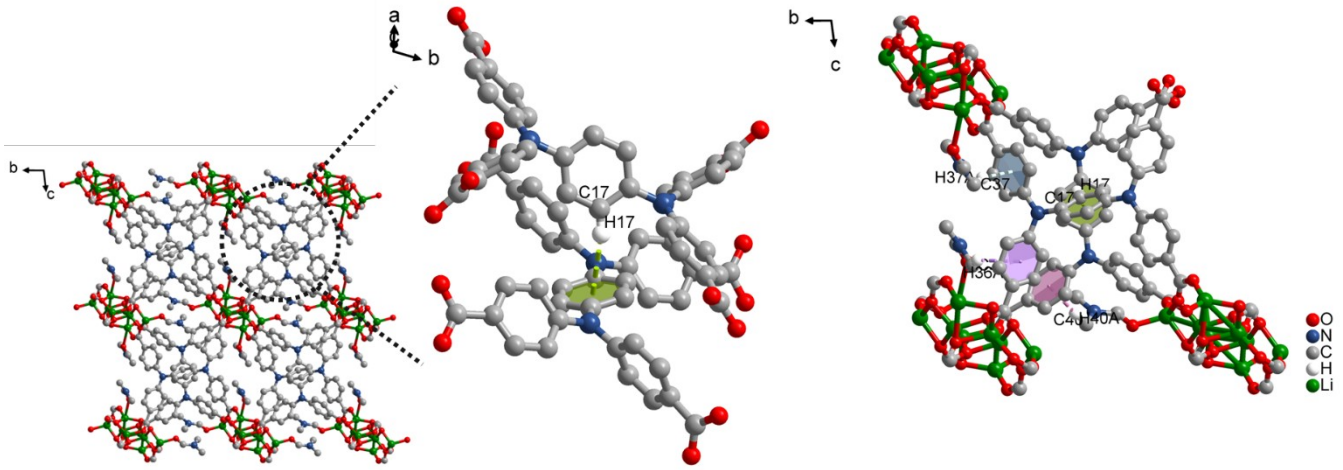

Figure S7. The C-H…π interactions in the three-dimensional framework of Li_8-MOF.

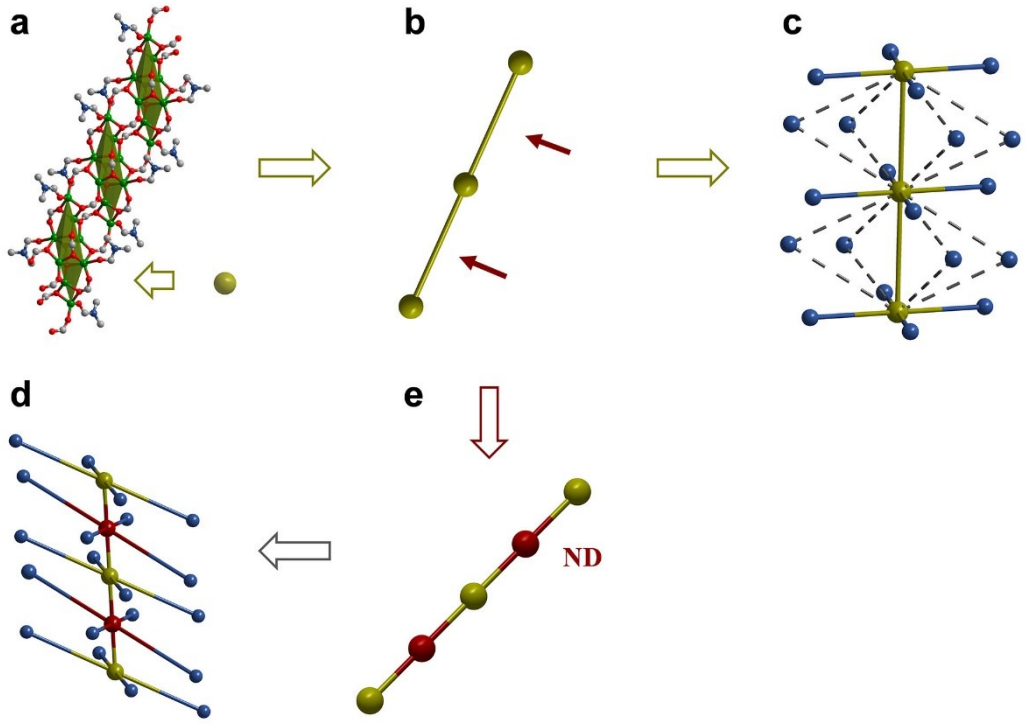

Figure S8. (a) Crystallographic representation of Li_8-based 1D chian. Topologically analysis of (b) cluster-based node, (c) cluster nodes coordinated, (d) cluster nodes and DNs coordinated, (e) Dummy nodes (DNs) are inserted into the centre of cluster nodes.

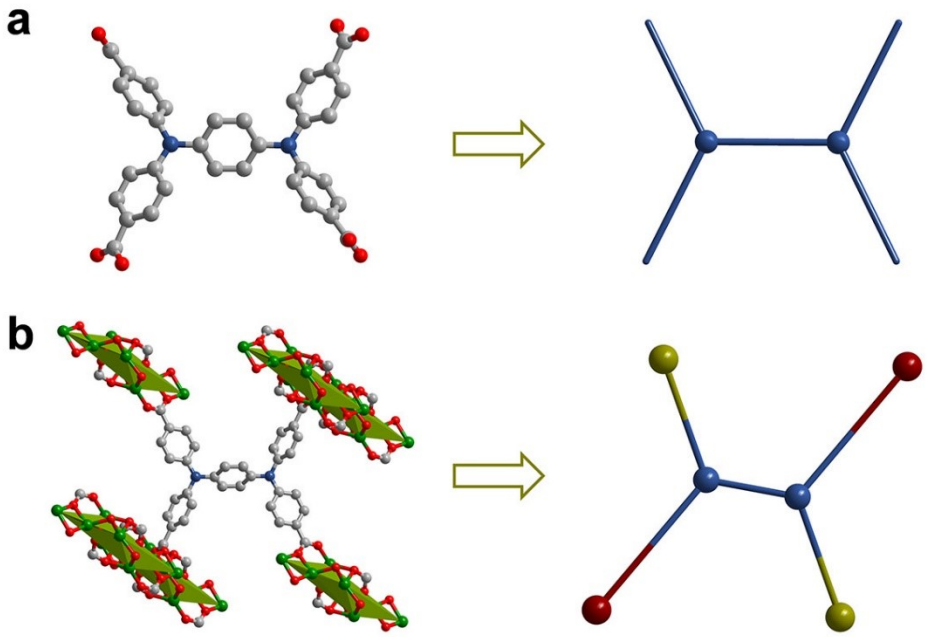

Figure S9. Crystallographic representation and topologically analysis of (a) $TCPPDA^{4-}$, (b) $TCPPDA^{4-}$ coordinated.

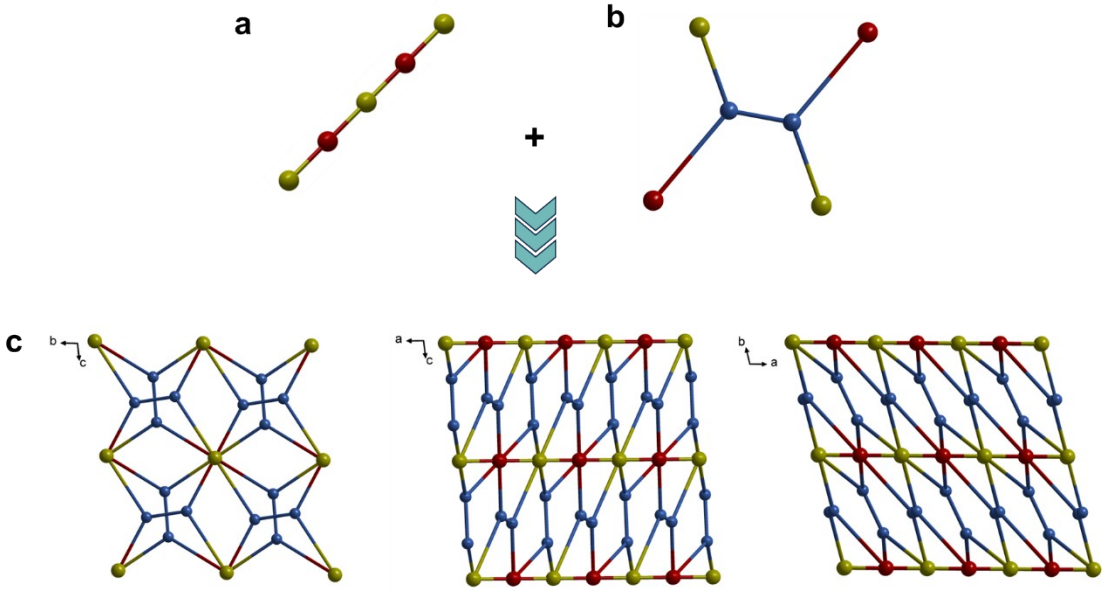

Figure S10. Topologically analysis for (a) 1D rod SBUs, (b) $TCPPDA^{4-}$, (c) ***a*** axis, ***b*** axis and ***c*** axis of Li_8-MOF.

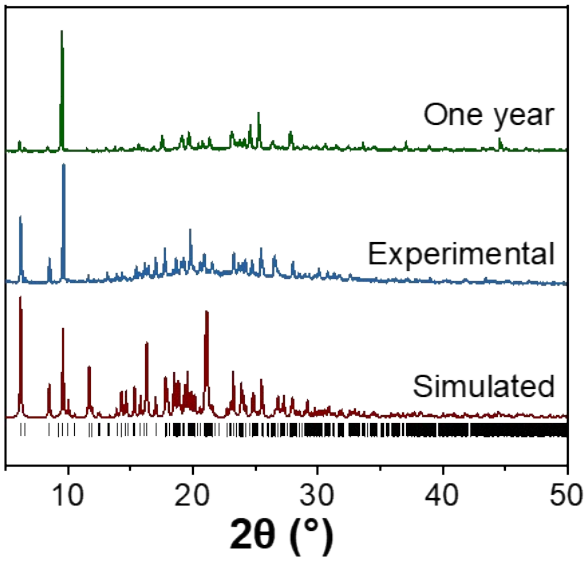

Figure. S11 PXRD patterns of Li_8-MOF stored in air for one year.

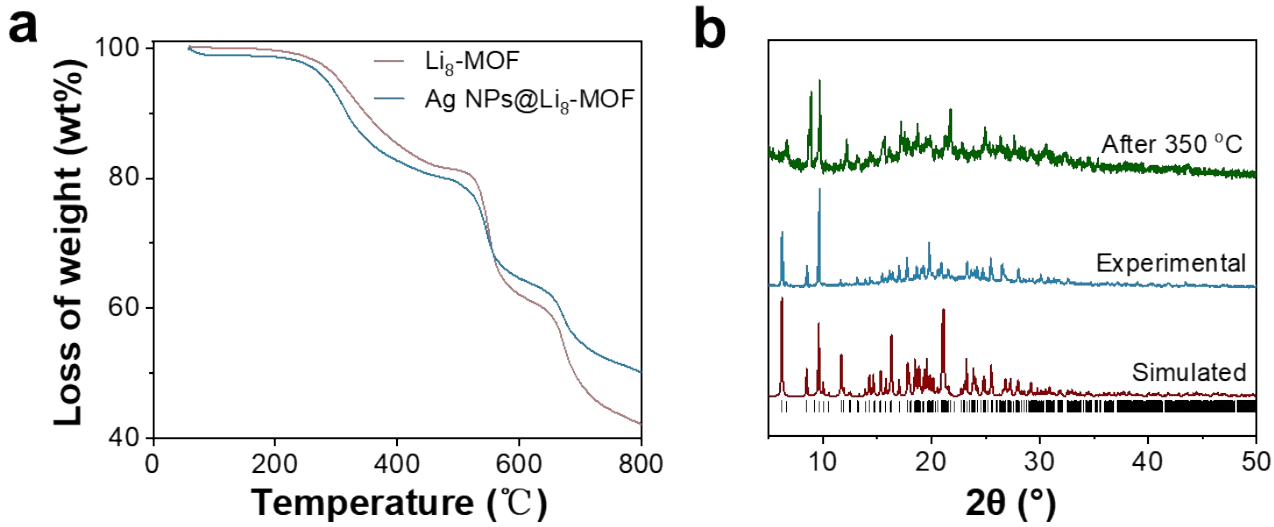

Figure. S12 (a) The TGA plots of Li_8-MOF and Ag NPs@Li_8-MOF in N_2 atmosphere. (b) The PXRD patterns of Li_8-MOF after being treated in a nitrogen atmosphere at 350 °C for 12 h.

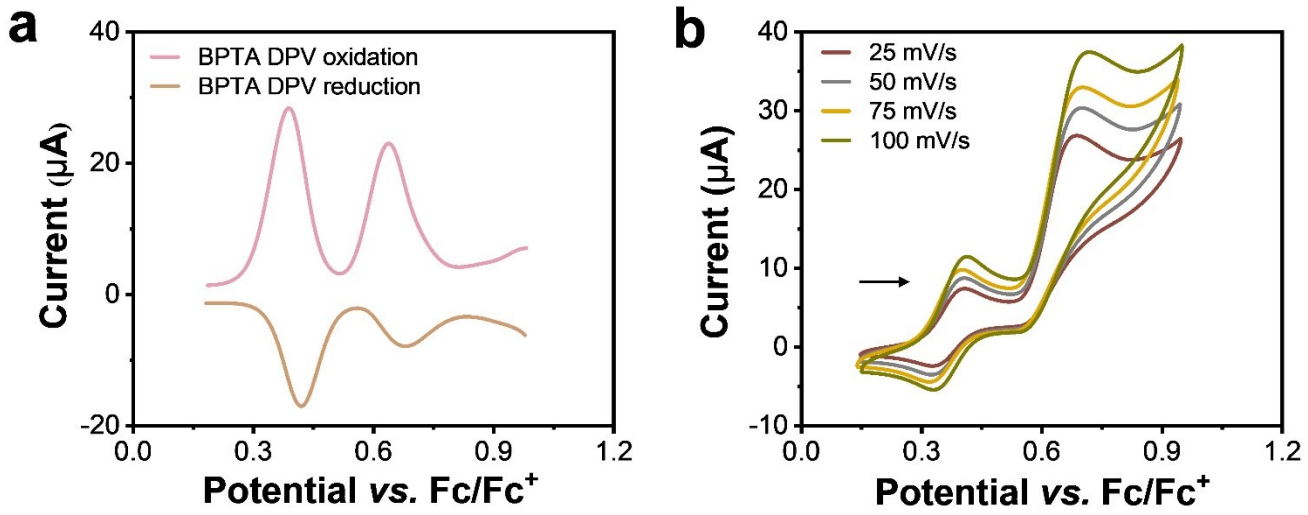

Figure. S13 Cyclic voltammograms of H_4TCPPDA ligand as the solution state in 0.1 M $(C_2H_5)_4N^+PF_6^-$ /DMF electrolyte. (a) oxidation and reduction peaks from the DPV, (b) scan rates of 25 -100 mV s^{-1}.

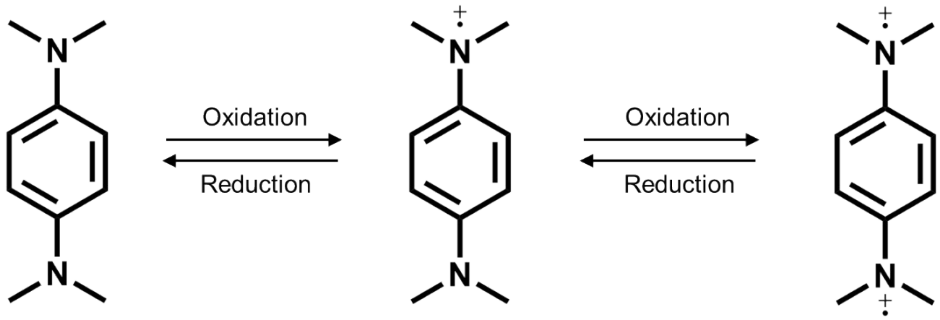

Figure. S14 Redox processes of H_4TCPPDA linker.

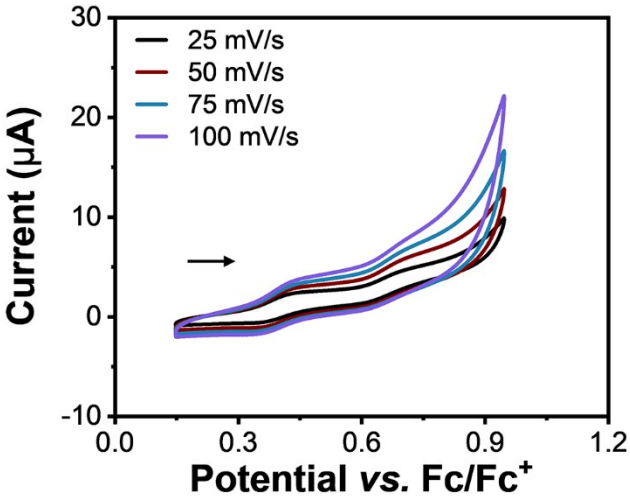

Figure. S15 Cyclic voltammograms of Li_8-MOF as the solid state in 0.1 M $(C_2H_5)_4N^+PF_6^-$ /DMF electrolyte at scan rates of 25 -100 mV s^{-1}.

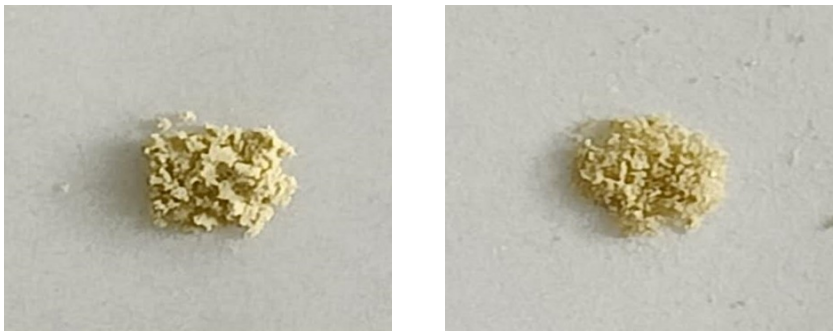

Figure. S16 Photographs of Li_8-MOF before (left) and after (right) submerged in a cyclohexane solution of I_2 for 12 hours.

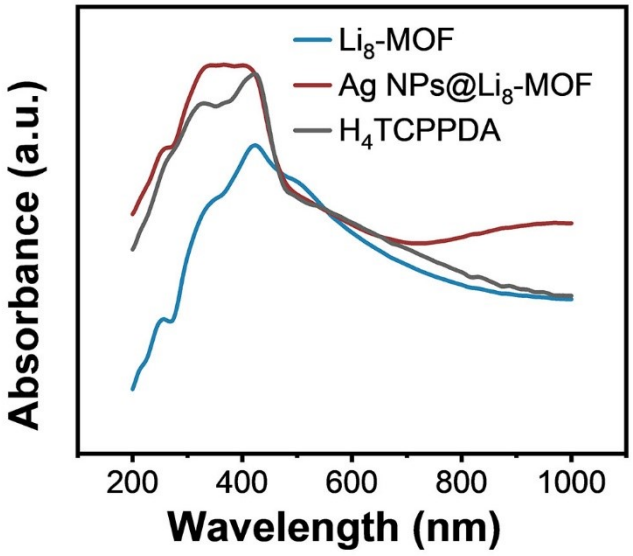

Figure S17. The UV-vis-NIR spectra of H_4TCPPDA, Li_8-MOF and Ag NPs@ Li_8-MOF.

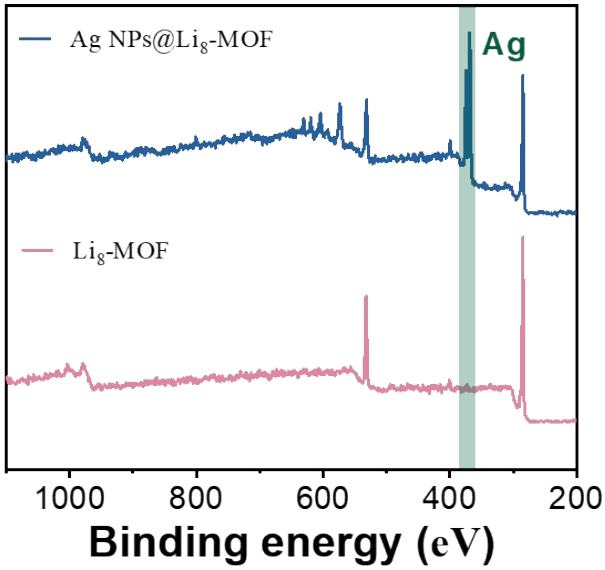

Figure S18. X-ray photoelectron spectra of Li_8-MOF, Ag NPs@Li_8-MOF (0.1 M $AgNO_3$ 8 h).

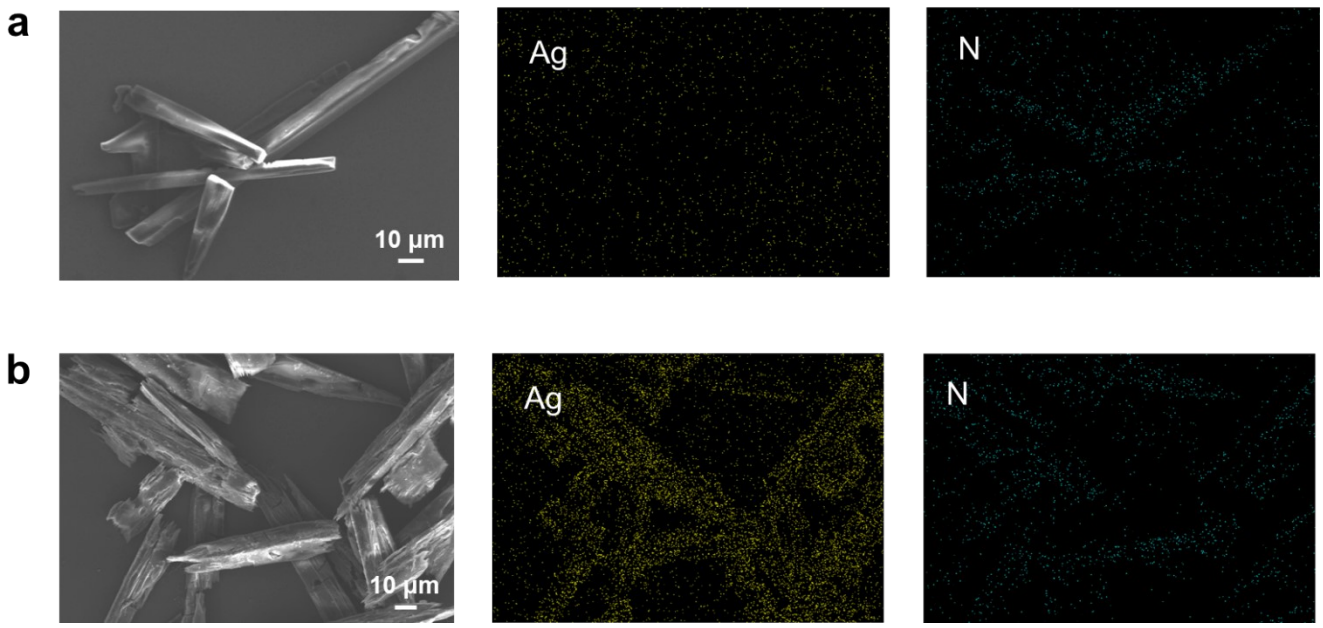

Figure. S19 Element mapping of Li_8-MOF and Ag NPs@Li_8-MOF (0.1 M $AgNO_3$ 8 h) under SEM/EDX.

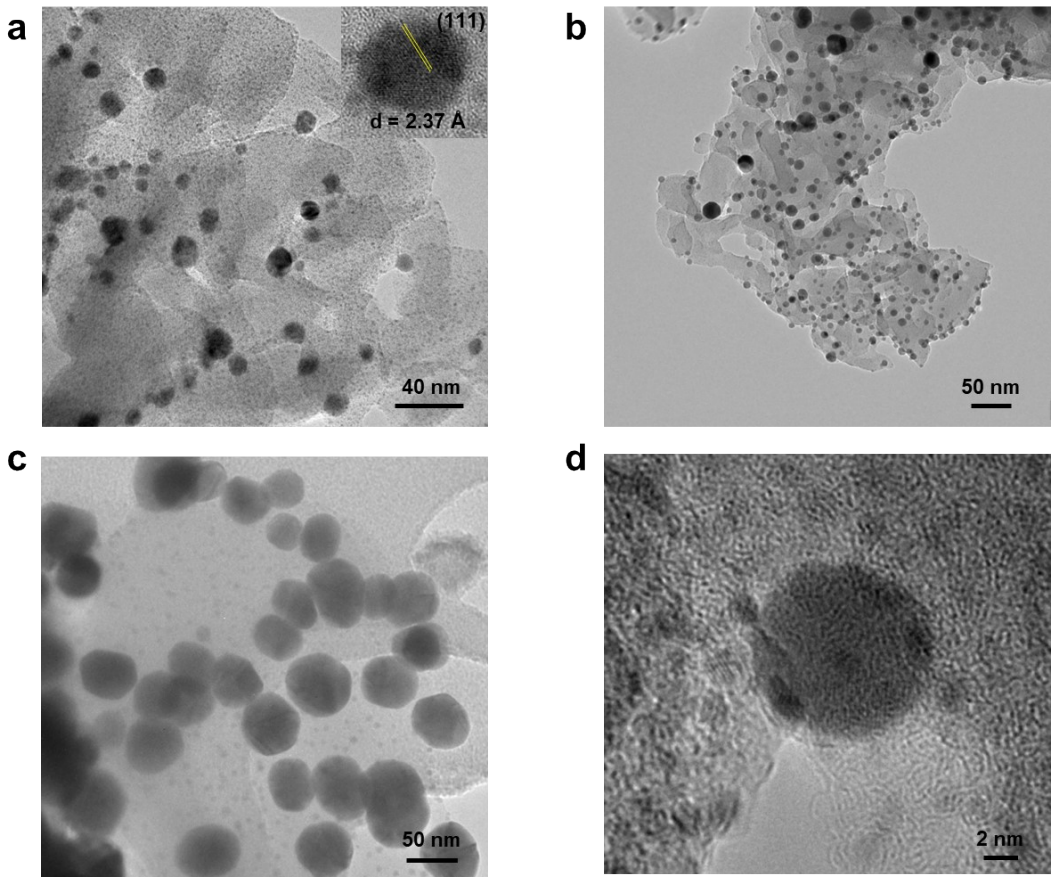

Figure. S20 HRTEM images of Ag NPs@Li_8-MOF (0.1 M $AgNO_3$ 8 h).

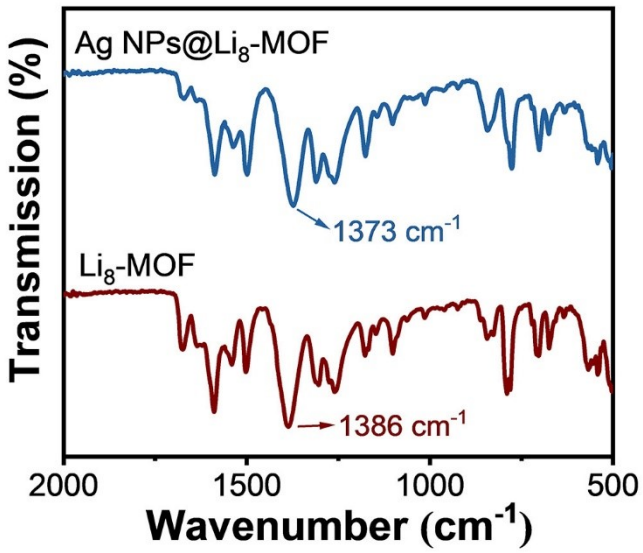

Figure S21. The IR spectra of Li_8-MOF and Ag NPs@Li_8-MOF . The shifted peak (around 1373 cm^{-1}) can be attributed to the vibration of NO_3^-.

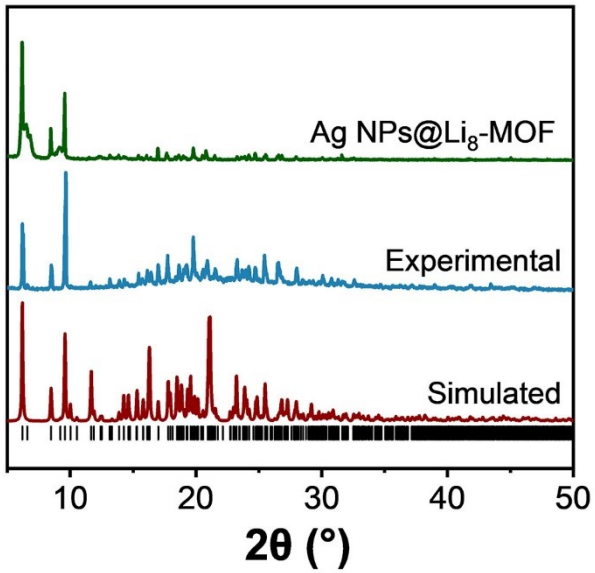

Figure. S22 The PXRD patterns of Ag NPs@Li_8-MOF resulting from immersion of the material in 0.01 M $AgNO_3$ for 8h in CH_3OH.

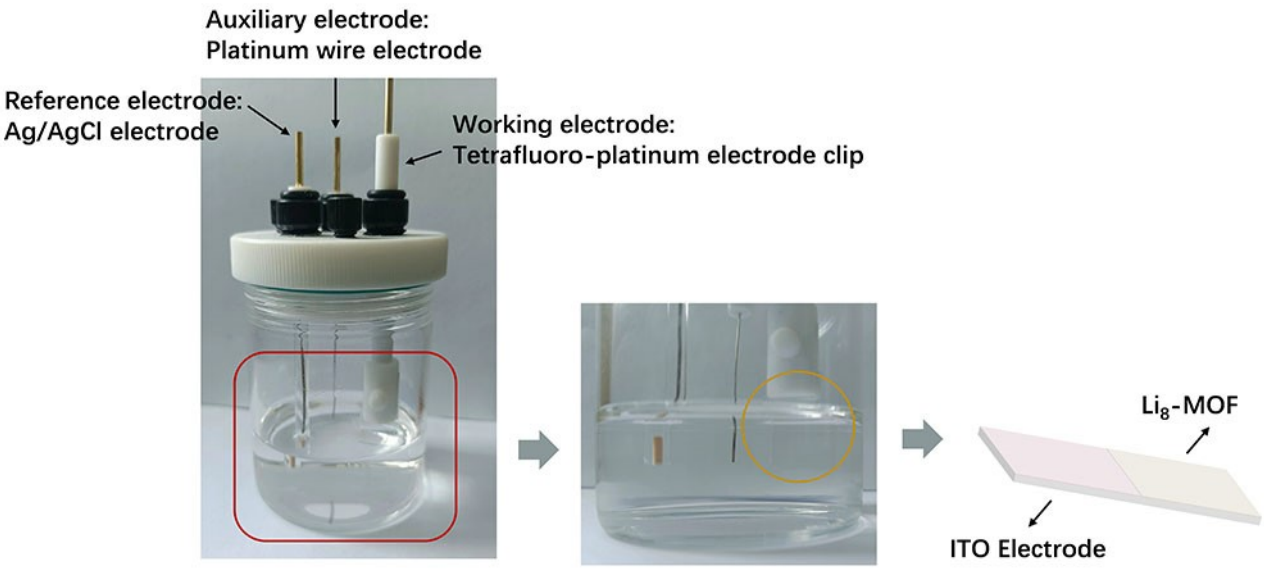

Figure. S23 Schematic diagram of electrochromic device.

References

[1] Z. Wei, Z.-Y. Gu, R. K. Arvapally, Y.-P. Chen, R. N. McDougald, Jr., J. F. Ivy, A. A. Yakovenko, D. Feng, M. A. Omary, H.-C. Zhou, Rigidifying Fluorescent Linkers by Metal–Organic Framework Formation for Fluorescence Blue Shift and Quantum Yield Enhancement. *J. Am. Chem. Soc.* **2014**, 136, 8269-8276.

[2] C. Gorbitz, What Is the Best Crystal Size for Collection of X-Ray Data? Refinement of the Structure of Glycyl-L-Serine Based on Data from a Very Large Crystal. *Acta Crystallogr. B* **1999**, 55, 1090-1098.

[3] G. Sheldrick, A Short History of Shelx. *Acta Cryst. A* **2008**, 64, 112-122.

[4] A. Spek, Single-Crystal Structure Validation with the Program Platon. *J. Appl. Crystallogr*. **2003**, 36, 7-13.

[5] D. Pugh, E. Ashworth, K. Robertson, L. C. Delmas, A. J. P. White, P. N. Horton, G. J. Tizzard, S. J. Coles, P. D. Lickiss, R. P. Davies, Metal–Organic Frameworks Constructed from Group 1 Metals (Li, Na) and Silicon-Centered Linkers. *Cryst. Growth Des.*, **2019**, 19, 487-497.

[6] B. F. Abrahams, M. J. Grannas, T. A. Hudson, R. Robson, A Simple Lithium(I) Salt with a Microporous Structure and Its Gas Sorption Properties. *Angew. Chem. Int. Ed.*, **2010**, 49, 1087-1089.

[7] S. B. Aliev, D. G. Samsonenko, M. I. Rakhmanova, D. N. Dybtsev, V. P. Fedin, Syntheses and Structural Characterization of Lithium Carboxylate Frameworks and Guest-Dependent Photoluminescence Study. *Cryst. Growth Des.*, **2014**, 14, 4355-4363.

[8] X. Zhao, M. S. Shimazu, X. T. Chen, X. H. Bu, P. Y. Feng, Homo-Helical Rod Packing as a Path Toward the Highest Density of Guest-Binding Metal Sites in Metal–Organic Frameworks. *Angew. Chem. Int. Ed.*, **2018**, 57, 6208-6211.

[9] B. F. Abrahams, C. J. Commons, A. D. Dharma, T. A. Hudson, R. Robson, R. W. S. Arlt, T. C. Stewart, K. F. White, Synthesis, structure and properties of coordination polymers formed from bridging 4-hydroxybenzoic acid anions. *CrystEngComm*, **2022**, 24, 1924-1933.

[10] A. V. Desai, V. Pimenta, C. King, D. B. Cordes, A. M. Z. Slawin, R. E. Morris, A. R. Armstrong, Conversion of a microwave synthesized alkali-metal MOF to a carbonaceous anode for Li-ion batteries. *RSC Adv.*, **2020**, 10, 13732-13736.